iJRASET
International Journal For Research in Applied Science and Engineering Technology

INTERNATIONAL JOURNAL FOR RESEARCH

IN APPLIED SCIENCE & ENGINEERING TECHNOLOGY

Volume: 11 **Issue:** III **Month of publication:** March 2023

DOI: https://doi.org/10.22214/ijraset.2023.49504

www.ijraset.com

Call: 08813907089 | E-mail ID: ijraset@gmail.com

International Journal for Research in Applied Science & Engineering Technology (IJRASET)
ISSN: 2321-9653; IC Value: 45.98; SJ Impact Factor: 7.538
Volume 11 Issue III Mar 2023- Available at www.ijraset.com

Effective Utilization of Available PEV Battery Capacity for Mitigation of Solar PV Impact and Grid Support with Integrated V2G Functionality

Mr. Vakeel Sridhar[1], Mr. S Radha Krishna Reddy[2]
[1]*PG Scholar in the Dept. of Electrical & Electronics Engineering, in Holy Mary Institute of Technology & Science, Bogaram (V), Medchal District, Hyderabad, India*
[2]*Professor in the Dept. of Electrical & Electronics Engineering, in Holy Mary Institute of Technology & Science, Bogaram (V), Medchal District, Hyderabad, India*

Abstract: ***Utilizing battery storage devices in plug-in electric vehicles (PEVs) for grid support using vehicle-to-grid (V2G) concept is gaining popularity. With appropriate control strategies, the PEV batteries and associated power electronics can exploited for solar photovoltaic (PV) impact mitigation and grid support. However, as the PEV batteries have limited capacity and the capacity usage is also constrained by transportation requirements, an intelligent strategy is necessary for an effective utilization of the available capacity for V2G applications. In this paper, a strategy for an effective utilization of PEV battery capacity for solar PV impact mitigation and grid support is proposed. A controllable charging/ discharging pattern is developed to optimize the use of the limited PEV battery capacity to mitigate PV impacts, such as voltage rise during midday or to support the evening load peak. To ensure an effective utilization of the available PEV battery capacity when used for travel (which is the main usage of the PEVs) or when interventions in the charging operation is caused by passing clouds, a strategy for dynamic adjustments in PEV charging/discharging rates is proposed. The effectiveness of the proposed strategy is tested using a real distribution system in Australia based on practical PV and PEV data.***

Keywords: Charging/discharging control, distribution network support, plug-in electric vehicles (PEVs), solar photovoltaic (PV) impact, vehicle-to-grid (V2G).

I. INTRODUCTION

This VEHICLE-TO-GRID (V2G) concept is becoming increasingly attractive for supporting the electric grid [1]–[9] from the stored energy in PEV batteries. PEVs are typically charged from the grid when people come back from work in the evening. Such collective charging can impose an additional burden [10]–[12] on the distribution system. However, with an increasing level of solar photovoltaic (PV) penetration in the distribution networks, this situation could be exploited as an opportunity to support a high level of solar PV penetration. Solar PV resources produce power at the peak level during midday. At this time, the residential feeder demand is typically lower compared to the evening peak. The PV output exceeding the local demand at the point of common coupling (PCC) of the PV inverter has to be injected into the grid and will produce a reverse directional power flow and voltage rise. These issues have been reported in [13] and [14] as major concerns in increasing the PV penetration level. Active power curtailment has been proposed in [15] to limit the voltage rise problem which makes the overall economics of a solar PV installation project less attractive. The consumption of reactive power has been proposed to reduce the voltage rise problem in [16], however, this will create a high reactive power flow and increased power loss in the feeder. Moreover, as distribution networks are constructed using different combinations of overhead and underground cables with high *R/X* ratio, this method may not be very effective due to the low sensitivity of voltage with reactive power. The integration of storage devices with solar PV systems can be an attractive solution in this case to store the surplus energy from solar PV by charging the batteries.

The number of electric vehicles sold each year is increasing due to the variety of types and models brought to market by automobile manufacturers. Although commercial electric vehicles are not designed with comprehensive V2G functionality at the moment, this may be available as an optional feature in near future at extra cost. Studies show that these vehicles are on travel only during a small portion of the day and the rest of the time these vehicles are in parked position [17]. The statistics presented in [18] show that the probability of a PEV to be parked anywhere during the midday period is over 0.9 and the probability for it to be parked at home is over 0.5 for urban and rural weekday or weekend day.

Further, it is likely in the developed countries that there are two cars in a household, one of which may be parked at home most of the time. PEVs can be plugged into the grid using a bidirectional charger while in a parked position to act as a storage device for solar PV systems. Similar with the stationary storage devices used with PV inverters, the PEVs can act to limit the voltage rise problem at midday by consuming power to charge the PEV battery and hence can contribute to the increase of PV penetration level in the distribution grid which would otherwise be limited by the high PV penetration problems. The stored energy in those PEV batteries can support the distribution feeder during evening peak by injecting power to the local PCC so that less power is imported through the feeder to reduce the stress on the grid. However, it is to be noted that the usage of PEV battery for the grid ancillary support can contribute to the loss of its cycle life and may cause a need for an early battery replacement.

The effectiveness of the V2G concept for mitigating PV impacts and grid support will depend on how the PEV battery capacity is utilized. The reverse power flow and voltage rise impact of PV will vary mainly depending on the sun irradiance level and the load demand (active and reactive power), and will be at the most severe state in the midday when PV power is at the peak level and load demand is the lowest. Therefore, it would be more effective to charge the PEV battery at the highest rate in the midday and at lower rates before and after the midday as compared to charging with a constant rate all the time. Similarly, it would be wise to discharge the PEV battery at the highest rate during the maximum peak load period and at lower rates before and after. As the PEV battery will have a limited capacity, the charging/discharging rates will have to be such that the capacity is neither left unused nor finished earlier than the intended period of operation. The use of a separate energy storage device for the mitigation of PV and PEV impacts is reported in [19] and [20]. Instead of using a separate battery, PEV battery is used in [21] for mitigation of voltage rise caused by PV. In a previous work, Alam *et al.* [22] have developed a strategy for the effective usage of the battery capacity integrated with rooftop PV systems for PV impact mitigation and evening peak load support. As the PEV battery capacity is also limited in nature and can also experience intermittencies due to incidental travels, it would be worthwhile to develop a control strategy for effective usage of PEV batteries for PV applications. The contribution of this paper is to develop a wise strategy for charging/discharging of the PEV battery to effectively exploit the opportunities of the V2G concept for mitigating the voltage rise impact of solar PV and for providing the evening peak load support.

The main contributions of the proposed strategy are as follows.

1) To make the PEV batteries consume the highest amount of surplus PV power when the PV impact is most severe.
2) To generate the highest amount of power from the PEV batteries when the maximum demand appear during the evening peak.
3) The dynamic adjustment feature of the PEV charging/discharging currents to account for the interventions in charging/discharging operation caused by travels and passing clouds to ensure an effective utilization of the available battery capacity.

Also, the paper proposes an intelligent strategy for the returning vehicles after work to be charged in the late night/early morning in a controlled manner to coincide the PEV charging load with the customer minimum load so that stress on the distribution system is reduced. Section II of the paper describes the charging/discharging rate determination method using the mathematical formulation of capacity constraints, usage pattern, and charging/ Discharging rate adjustment of the PEV battery. Section III tests the performance of the proposed strategy using a real distribution network model. Section IV concludes the paper summarizing the overall contributions of the paper.

II. PEV BATTERY CONTROL STRATEGY FOR PV IMPACT MITIGATION AND GRID SUPPORT

A conceptual diagram showing a parked PEV connected to a PCC of a PV system, household loads and the distribution grid is shown in Fig. 1(a). The surplus power from the PV system will be consumed by the PEV battery to mitigate the impacts of excess PV power, such as reverse power flow, voltage rise, etc. The stored energy in the PEV battery can be used for grid support during grid peak load period, e.g., in the evening, and when no PV is present, e.g., during cloudy period. A number of PEVs connected to the feeder at the same time, as shown in Fig. 1(b), can bring considerable benefits for the whole feeder and upstream network in terms of voltage rise mitigation and voltage support. It is to be noted that at a given instant of time, all the PEVs in a feeder may not be present as they are out for travel as shown using dashed rectangles in Fig. 1(b). This would be the case particularly during the day time. However, the remaining amount of PEVs parked at home can still be used for PV impact mitigation. As PEV battery capacity is limited in nature, a wise strategy to effectively utilize this limited capacity would be necessary for network support. A charging/discharging control strategy leading to an effective utilization of the PEV battery is developed below.

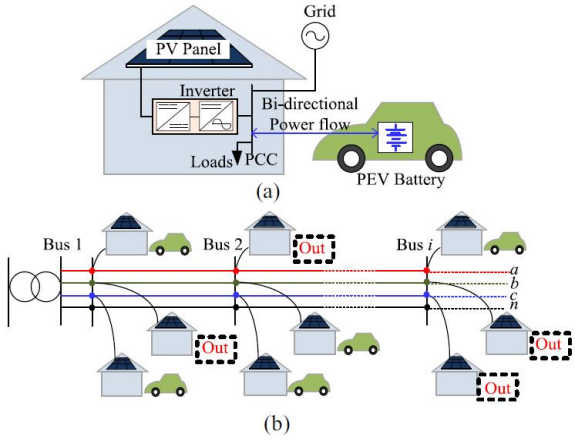

Fig. 1. PEV for PV impact mitigation and grid support. (a) Connection of a PEV with the PCC. (b) Number of PEVs connected to the feeder.

A. Determination of Charging/Discharging Rate for Effective Utilization of PEV Battery Capacity

Assume that the PEV will have to be charged in *T*Chg hours during the surplus PV power period over the day, as shown in Fig. 2(a). This period can be determined from the historical load and PV generation profile. The values of the PEV charging current are controlled during this period based on a user-defined pattern to effectively utilize the PEV battery capacity for PV impact mitigation. Typically, under a clear-sky condition, PV output will reach its peak during the midday, increasing from a zero value at the sunrise and again will decrease to a zero value at the sunset. Therefore it would be wise to charge the PEV battery at a higher rate during the midday period as compared to the charging rates during the morning and afternoon periods. Fig. 2(b) shows a trapezoidal pattern is used to consider this scenario in the PEV charging current control. To ensure that the PEV battery capacity is not left unused or the battery is not overcharged, the PEV charging current is controlled at any given time instant *k* according to

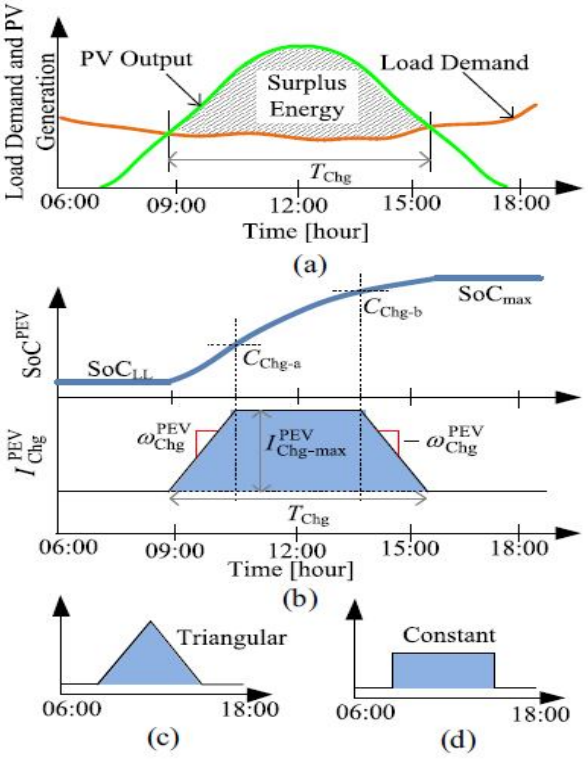

Fig. 2. Development of a PEV charging current control strategy. (a) Load and PV generation profile. (b) Control of PEV charging current in relation toPEV SoC. (c) Triangular charging profile. (d) Constant charging profile.

$$I_{\text{Chg}}^{\text{PEV}}(k) = \begin{cases} I_{\text{Chg}}^{\text{PEV}}(k-1) + \omega_{\text{Chg}}^{\text{PEV}}\Delta t, & \text{if } \text{SoC}^{\text{PEV}}(k-1) \le C_{\text{Chg-a}} \\ I_{\text{Chg-max}}^{\text{PEV}}, & \text{if } C_{\text{Chg-a}} < \text{SoC}^{\text{PEV}}(k-1) < C_{\text{Chg-b}} \\ I_{\text{Chg}}^{\text{PEV}}(k-1) - \omega_{\text{Chg}}^{\text{PEV}}\Delta t, & \text{if } \text{SoC}^{\text{PEV}}(k-1) \ge C_{\text{Chg-b}} \\ 0, & \text{if } \text{SoC}^{\text{PEV}}(k-1) \ge \text{SoC}_{\text{max}}^{\text{PEV}} \end{cases} \quad (1)$$

where *I*PEV Chg is the PEV charging current (ampere); *ω*PEV Chg is the rate of change of charging current (ampere per time instant) to follow the user defined charging profile; _*t* is the time difference between two time instants; SoCPEV is the SoC of PEV battery; *C*Chg-a and *C*Chg-b are the two thresholds of SoC (in per unit) specifying the shape of the user defined charging profile.

The values of *I*PEV Chg-max and *ω*PEV Chg can be determined from a system of nonlinear equations given below in (2), developed based on the geometric relationships of the charging profile during the period *T*Chg in Fig. 2(b). The amount of charge accumulated during the period when the charging rate increases from zero to the maximum value can be obtained using the expression of the area of a triangle. The upper expression in the right hand side of (2) is then obtained by equating this amount with the amount of charge obtained using points *C*Chg-a and SoCLL on the SoC curve in Fig. 2(b). The amount of charge accumulated during the period when the charging rate is constant can be obtained using the expression of the area of a rectangle. The lower expression in the right hand side of (2) is then obtained by equating this amount with the amount of charge obtained using points *C*Chg-a and *C*Chg-b on the SoC curve in Fig. 2(b)

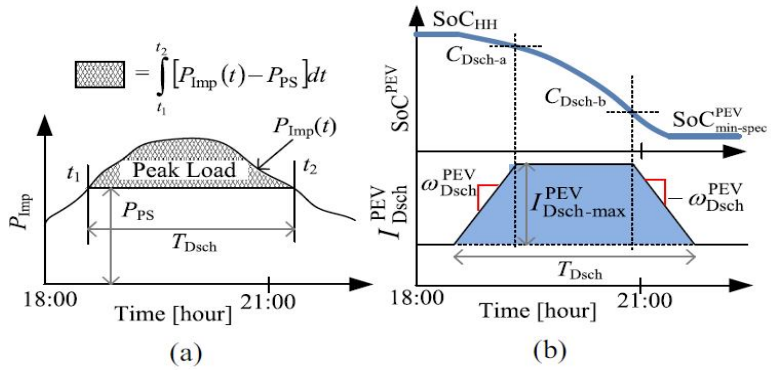

Fig. 3. Development of PEV battery discharge strategy. (a) Determination of *T*dsch. (b) Control of PEV discharging current in relation to PEV SoC.

$$0 = \begin{cases} \dfrac{0.5\left(I_{\text{Chg-max}}^{\text{PEV}}\right)^2}{\omega_{\text{Chg}}^{\text{PEV}} \times F_{\text{Time}}} - C^{\text{PEV}}\left(C_{\text{Chg-a}} - \text{SoC}_{\text{LL}}\right) \\ \left(T_{\text{Chg}} - \dfrac{2I_{\text{Chg-max}}^{\text{PEV}}}{\omega_{\text{Chg}}^{\text{PEV}} \times F_{\text{Time}}}\right) \times I_{\text{Chg-max}}^{\text{PEV}} - C^{\text{PEV}}\left(C_{\text{Chg-b}} - C_{\text{Chg-a}}\right) \end{cases}$$

(2)

where SoCLL is the SoC at the start of the charging operation; *C*PEV is the capacity of the PEV battery in Ah, *F*Time is a conversion factor to convert the unit of time to hour from the unit of time used in (1); if the unit of time in (1) is minute or second, *F*Time will be 60 or 3600, respectively. The limits *C*Chg-a and *C*Chg-b are obtained using user defined parameters *K*Chg-a and *K*Chg-b, respectively, that sets the proportions of the available capacity of the PEV battery to be spent during the time when the charging rate is increasing and when the charging rate is constant, as

$$C_{\text{Chg-a}} = \text{SoC}_{\text{LL}} + \left(\text{SoC}_{\text{max}}^{\text{PEV}} - \text{SoC}_{\text{LL}}\right) \times K_{\text{Chg-a}}$$
$$C_{\text{Chg-b}} = C_{\text{Chg-a}} + \left(\text{SoC}_{\text{max}}^{\text{PEV}} - \text{SoC}_{\text{LL}}\right) \times K_{\text{Chg-b}}. \quad (3)$$

The user defined variables *K*Chg-a and *K*Chg-b can be used to control the charging profile patterns. The trapezoidal pattern in Fig. 2(b) is obtained using *K*Chg-a = 0.25 and *K*Chg-b = 0.5.

The PEV charging profile can be switched to a triangular shape by setting *K*Chg-a = 0.5 and *K*Chg-b = 0, as shown in Fig. 2(c); a constant charging profile can be obtained by setting *K*Chg-a = 0.0 and *K*Chg-b = 1.0, as shown in Fig. 2(d). Discharging of the PEV battery is performed for peak load support in the evening when PV power is not available, while retaining a limited capacity in case there is a need for travel. This limited capacity depends on the distance for which the PEV will need to be able to run before the next charging. A peak-shaving strategy is adopted for discharge operation where the PEV battery will inject power depending on the available capacity in the PEV battery. The discharging period can be obtained from a reference demand curve, as shown in Fig. 3(a), derived from historical demand curves of the customer household where the PEV will be plugged in. If discharge operation is performed for *T*Dsch hours using a peak shaving mode, then the following expression will be true:

$$\int_{t_1}^{t_2} [P_{\text{Imp}}(t) - P_{\text{PS}}]dt - C^{\text{PEV}} \times \left(\text{SoC}_{\text{HH}} - \text{SoC}_{\text{min-spec}}^{\text{PEV}}\right) \times V_{\text{batt}}^{\text{PEV}} = 0$$
$$t_2 - t_1 = T_{\text{Dsch}}, \left(P_{\text{Imp}}(t) - P_{\text{PS}}\right) \geq 0 \qquad (4)$$

where *P*Imp is the power import from the grid by the load demand, *P*PS is the threshold power for peak-shaving operation, SoCHH is the SoC at the start of the discharge period, SoCPEV min-spec is the user specified minimum SoC of the PEV battery. The value of *P*PS that satisfies (4) is used to derive *T*Dsch. To effectively utilize the PEV battery capacity in the discharge operation, the PEV discharge current is controlled in such a way that the highest discharging rate appears during the period of the maximum evening peak load, and lower in the periods before and after that, as shown in Fig. 3(b). At a given *k*th instant, the discharge current is controlled as

$$I_{\text{Dsch}}^{\text{PEV}}(k) = \begin{cases} I_{\text{Dsch}}^{\text{PEV}}(k-1) + \omega_{\text{Dsch}}^{\text{PEV}}\Delta t, & \text{if } \text{SoC}^{\text{PEV}}(k-1) \geq C_{\text{Dsch-a}} \\ I_{\text{Dsch-max}}^{\text{PEV}}, & \text{if } C_{\text{Dsch-a}} > \text{SoC}^{\text{PEV}}(k-1) > C_{\text{Dsch-b}} \\ I_{\text{Dsch}}^{\text{PEV}}(k-1) - \omega_{\text{Dsch}}^{\text{PEV}}\Delta t, & \text{if } \text{SoC}^{\text{PEV}}(k-1) \leq C_{\text{Dsch-b}} \\ 0, & \text{if } \text{SoC}^{\text{PEV}}(k-1) \leq \text{SoC}_{\text{min-spec}}^{\text{PEV}}. \end{cases} \qquad (5)$$

The values of *I*PEV Dsch-max and ωPEV Dsch are obtained from a similar nonlinear system of equation as given in (2) by replacing the parameters related to the charging operation with the parameters related to the discharging operation. The PEV battery overcharge limit SoCPEV max can be obtained from the manufacturer specified maximum limit. The value of SoCPEV min-spec for a PEV battery will depend on how much energy will have to be retained for the travels before next charging opportunity. In this paper, the value of SoCPEV min-spec is obtained using the distance for which the PEV will need to be able to run before the next charging, as

$$\text{SoC}_{\text{min-spec}}^{\text{PEV}} = \text{SoC}_{\text{min}}^{\text{PEV}} + \frac{l_{\text{travel}} + \text{FE}_{\text{PEV}}}{C^{\text{PEV}} \times V_{\text{batt}}^{\text{PEV}}} \qquad (6)$$

where SoCPEV min is the manufacturer specified minimum SoC, *l*travel is the travel length before the next charging including any incidental travel (to hospital, police station, etc.) in km, and FEPEV is the PEV fuel economy in kWh/km. It is worth to consider that utilizing a PEV battery for customer load support using V2G functionality will increase the number of charging/discharging cycles and may impact the battery life.

B. Adjustment of PEV Battery Charging/Discharging Current to Account for Intermittent Events

PEV battery will be charged from surplus solar PV power which is practically intermittent due to the dependency on the solar irradiance level. If the solar irradiance is not available for a certain amount of time, the PEV battery cannot be charged. Also, if the PEV is used for any travel within the charging period, the PEV capacity will be depleted. To account for this, the charging rate will have to be adjusted during the periods when surplus PV power is again available. The adjustment of PEV battery charging current is performed based on a reference SoC profile that is obtained using (1). If there is a deviation between the reference SoC and the actual SoC, then adjustment is made to make up for the difference as

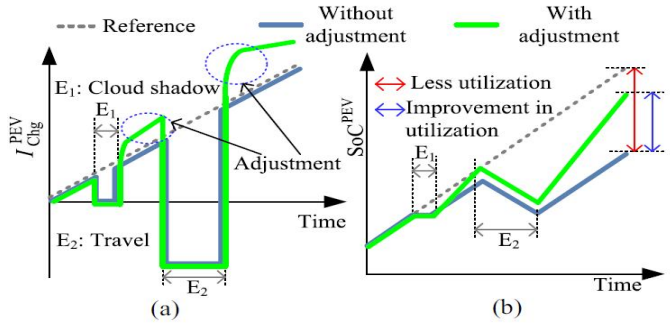

Fig. 4. Adjustment of PEV charging current for better utilization of PEV battery capacity. (a) PEV charging current. (b) PEV SoC.

$$I^{\text{PEV}}_{\text{Chg-adj}}(k) = I^{\text{PEV}}_{\text{Chg}}(k) + \Delta I^{\text{PEV}}_{\text{Chg-adj}}(k)$$
$$\Delta I^{\text{PEV}}_{\text{Chg-adj}}(k) = \frac{C^{\text{PEV}} \times F_{\text{Time}} \times \left\{\text{SoC}^{\text{PEV}}_{\text{ref}}(k) - \text{SoC}^{\text{PEV}}_{\text{act}}(k)\right\}}{T_{\text{adj}}}$$
$$\text{SoC}^{\text{PEV}}_{\text{act}}(k) = \text{SoC}^{\text{PEV}}_{\text{act}}(k-1) + \frac{I^{\text{PEV}}_{\text{Chg}}(k) \times \Delta t}{C^{\text{PEV}} \times F_{\text{Time}}} \qquad (7)$$

where *I*PEV Chg-adj*(k)* is the adjusted charging rate, _*I*PEV Chg-adj*(k)* is the amount of adjustment, and *T*adj is a time period for accomplishing the adjustment for minimizing the deviation between the actual SoC, SoCPEV act and the reference SoC, SoCPEV ref . To account for the deviation between the actual SoC and the reference SoC, the PEV charging current may experience high step changes. A rate-limiter is deployed to avoid a high step change in PEV charging current, as.

$$I^{\text{PEV}}_{\text{Chg-adj-R}}(k) = I^{\text{PEV}}_{\text{Chg-adj-R}}(k-1) + \frac{I^{\text{PEV}}_{\text{Chg-adj}}(k) - I^{\text{PEV}}_{\text{Chg-adj-R}}(k-1)}{n_{\text{step}}} \qquad (8)$$

where *I*PEV Chg-adj-R is the rate limited PEV charging current and *n*step is the number of steps to limit the rate. If such an adjustment is made in the charging rate, an effective utilization of the PEV battery capacity can be accomplished. Fig. 4 shows the PEV battery SoC profile that experiences intermittency due to cloud shadow and unavailability of the PEV battery due to an incidental travel. If no adjustment of the charging current is performed, PEV battery capacity is left unused. However, if an appropriate adjustment is carried out using (7), a better utilization of the PEV battery is possible.

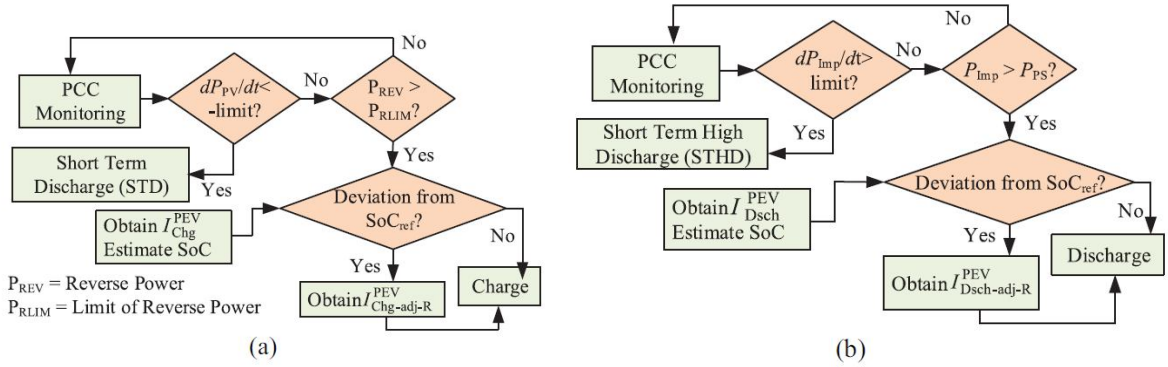

Fig. 5. Control of PEV battery for V2G application. (a) Charging operation. (b) Discharging operation.

Similar adjustments will have to be made for the PEV battery discharge current to account for the deviation between the reference SoC obtained using (5), and the actual SoC. Such deviations can be caused by any incidental travel related capacity discharge, any event requiring a short term high discharge, such as supporting a voltage dip, etc.

C. Control Strategy for PEV Charging/Discharging

The control flowchart for the proposed strategy is shown in Fig. 5. The PEV management system continuously monitors the PCC net power *P*PCC. If a reverse power flow at the PCC, greater than a threshold is experienced, the PEV battery is charged with the surplus PV power. However, if a sudden decrease in PV power is found, the PEV battery is put into a short-term discharge (STD) mode and discharged to provide compensation for sudden decrease in PV output, as shown in Fig. 5(a). To account for any deviation between the reference SoC and the actual SoC of the PEV battery, the charging current is adjusted. Such deviations can be caused by a travel causing battery capacity discharge, unavailability of surplus PV power due to cloud shadow, or discharging of PEV battery in STD mode. Charging operation is performed using the adjusted and rate-limited charging current command. PEV discharge operation is performed to provide a peak load support. If the power import from grid, *P*Imp, exceeds the threshold of peak-shaving load, *P*PS, discharge operation is performed. In case there is an event that causes a sudden increase in *P*Imp, such as a motor start, the PEV battery is put into a short-term high discharge (STHD) mode, as shown in Fig. 5(b). To account for the deviation in SoC created by the difference between the reference demand curve and the actual demand, the STHD operation, and any travel, the discharge rate is adjusted and rate-limited before issuing the discharge command.

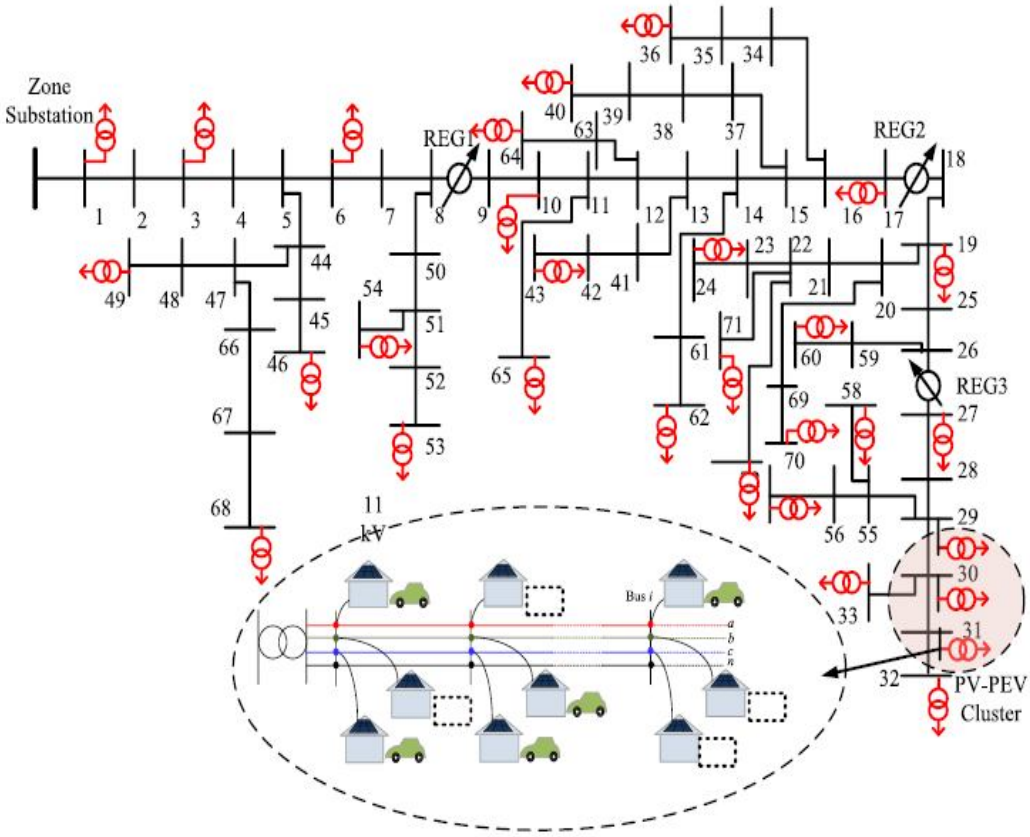

Fig. 6. Practical distribution system in Australia.

III. CASE STUDIES

A distribution network containing medium voltage (MV) and low voltage (LV) feeders has been extracted from a New South Wales distribution system in Australia to investigate the applicability of the proposed mitigation strategy. This is an 80 km long 11 kV rural network containing over 70 11 kV nodes. A single line diagram of the network is shown in Fig. 6. One of the LV feeders is shown in detail in a dashed circular shape.

It is a 0.4 kV 3 phase LV feeder constructed using a 7×3.00 mm all aluminum conductor (7/3.00 AAC) with *R/X* ratio of 2.5 (typically Australian LV networks have *R/X* ratio over 1.0 and can be higher than 4.5 with LV aerial bundled conductor). The feeder supplies power to 18 customers, 6 customers per phase. Although, a balanced customer distribution has been considered in this paper, unbalanced customer distribution is observed in LV feeders in Australia and this can pose new challenges for balancing in the presence of PV and PEV.

Specifications of the LV feeder used for simulation are presented in Table I. For the analysis of PV and PEV impacts, the LV feeders connected to bus 29, 30, and 31 have considered forming a cluster where all the customers have rooftop PV and PEV.

The load profile data is obtained from a real load demand curve captured by an Australian distribution utility and the PV data corresponds to a PV output profile captured by the Commonwealth Scientific and Industrial Research Organisation (CSIRO) on the February 5, 2011. The PV system sizes at the residential households were limited within 4 kW and operated at unity power factor. PEVs are simulated using specifications given in Table II, based on a Nissan Leaf [23]. PEV batteries are modeled by mapping the nonlinear relationship between SoC and battery voltage incorporating the effect of internal resistance [22] to account for the round-trip efficiency of the battery, which is 77%–81% for a typical lead-acid battery [24]. The 0.95 charger efficiency [25] is considered for the on-board charger of the PEV which is used normally for home charging and it does not include battery losses. The user specified minimum SoC of the PEV battery is determined using (6) based on a 30 km per day travel and an incidental 10 km travel. The 30 km per day travel assumption is based on the driving habit statistics reported in [26]. Several simulation scenarios have been set up for the analysis of the PV impact mitigation and grid support by PEV. To mitigate the voltage rise impact using the battery storage device of the PEV battery, the PEV needs to be parked at home.

According to the statistics presented in [18], the probability of a PEV to stay at home during the daytime of a weekday is over 0.5. Based on this, 50% of the PEVs, i.e., 27 out of 54 PEVs in the entire PV–PEV cluster are assumed to be parked and plugged in at home to be charged from the surplus PV power.

At first, a scenario is considered where none of the 50% of PEVs staying at home go for a travel during the daytime charging period, and therefore all the PEVs can be charged without any intervention. The load and PV output profile for a customer in the PV–PEV cluster is shown in Fig. 7(a), where the periods of charging and discharging are identified using *T*Chg and *T*Dsch, respectively. Using the PEV charging pattern in (1), obtained from the parameters based on (2) and (3), the power consumption profile for PEV battery charging is shown in Fig. 7(b).

The power consumed by the PEV battery increases from zero at the start of the reverse power flow period, reaches the peak level at the midday and decreases to zero at the end of the reverse power flow period. If the PEV battery is charged using a constant rate, then the power consumed by the PEV battery would be either a constant (based on the charging rate and battery voltage), or equal to the surplus PV power available at the PCC.

Fig. 7(b) shows the power profile of the PEV battery based on a constant charging rate and based on the proposed charging strategy. It is observed that at midday when surplus power is at its maximum and the PV impact is most significant, then the charging power with the proposed charging strategy (approximately 1.6 kW) is higher than that from the constant charging rate (approximately 1.0 kW). During the evening peak demand period, the load support using the proposed strategy is also higher than that from the constant discharge strategy.

TABLE I
DATA OF A TYPICAL AUSTRALIAN LOW VOLTAGE FEEDER

Feeder Length (metre)	240
Pole to Pole Distance (metre)	40
MV/LV Transformer	160 kVA, 3 ph
Maximum Load per Customer	2.2 kW at 0.95 PF (lag)
PV Size (kW)	4 kW
PV Module and Inverter Make	Kyocera /SMA Sunnyboy

TABLE II
PEV DATA USED FOR SIMULATION

PEV Make and Model	Nissan Leaf
Rated Battery Capacity	60 Ah/24 kWh
Voltage	364 V
PEV Fuel Economy	0.3 kWh/mile
Charger Efficiency	0.95

International Journal for Research in Applied Science & Engineering Technology (IJRASET)
ISSN: 2321-9653; IC Value: 45.98; SJ Impact Factor: 7.538
Volume 11 Issue III Mar 2023- Available at www.ijraset.com

IV. SIMULATION RESULTS

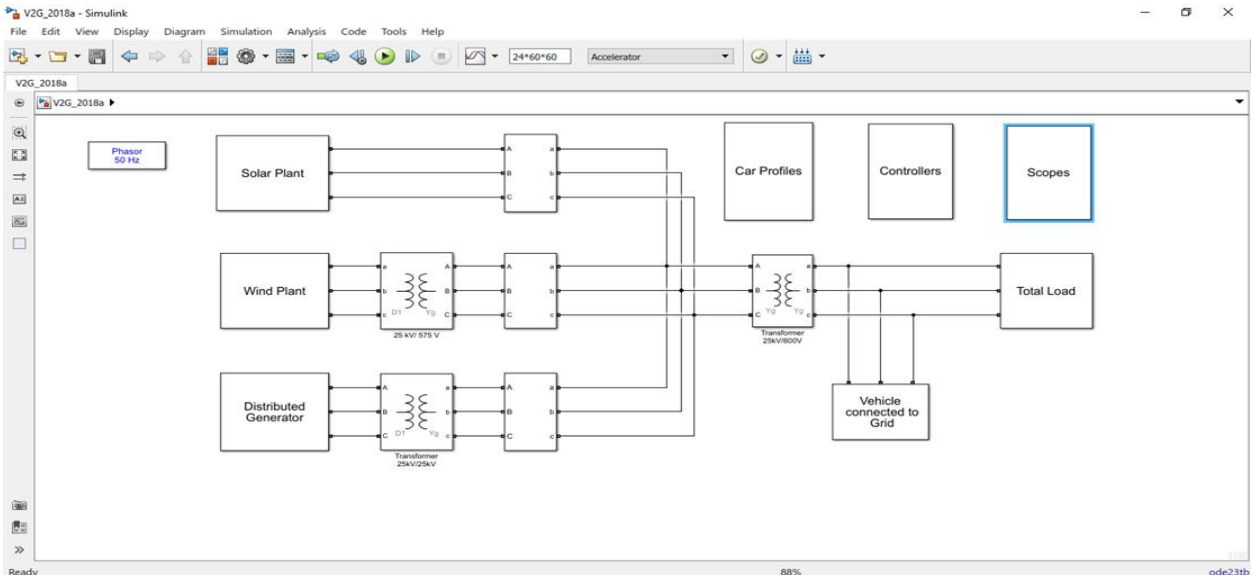

Fig7. V2G impact on grid for unbalanced Renewable energy sources.

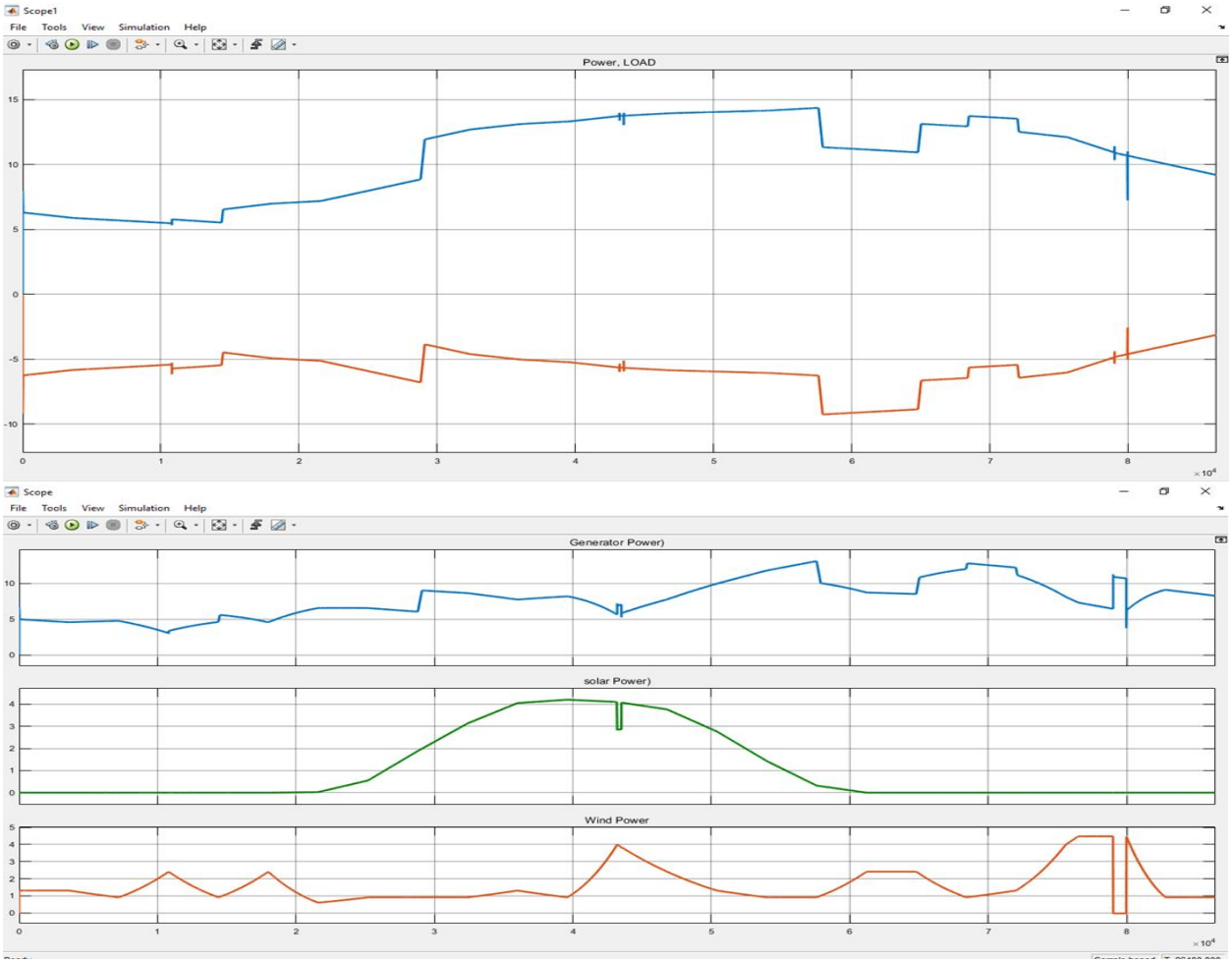

Fig9. PV impact mitigation and grid support using PEV battery. (a) Load demand and PV generation. (b) PEV storage power profile. (c) PEV SoC profile. (d) Voltage profile at the LV side of the MV/LV substation.

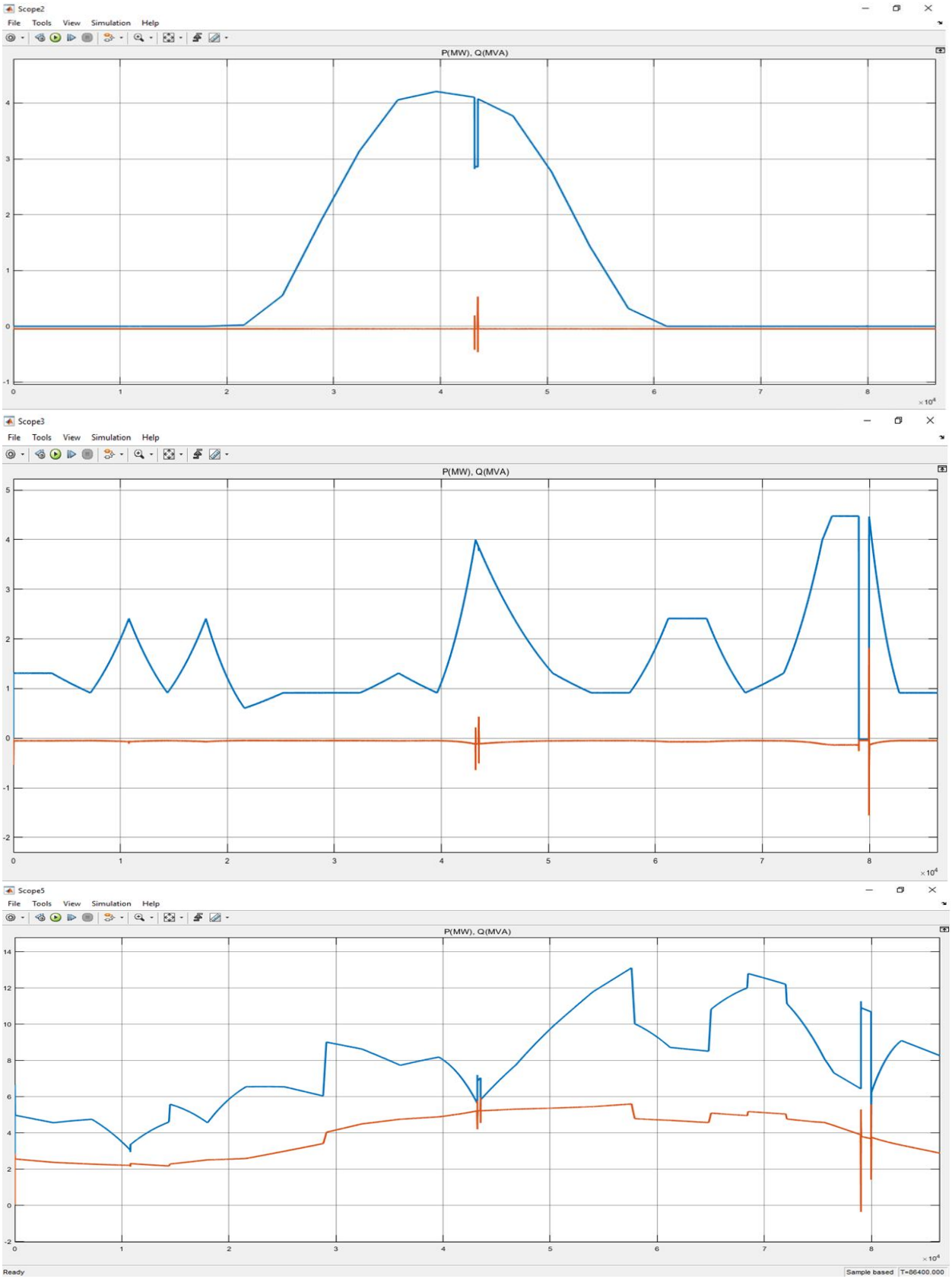

Fig10. PV impact mitigation and grid support using PEV battery when some of the PEVs are absent during a travel. (a) PEV storage power profile. (b) PEV SoC profile. (c) Voltage profile at the LV side of the MV/LV substation.

V. CONCLUSION

This paper has developed a charging strategy, to effectively store energy in the PEV batteries taking into account the limited PEV battery capacity, for the mitigation of voltage rise and reverse power flow caused by surplus solar PV power during midday. The paper has also proposed a discharging strategy for the use of the stored energy in PEV batteries for the distribution network voltage support, especially during evening peak load period, while ensuring that there is sufficient remaining capacity in the batteries in case there is a need for travel prior to the next charging event. The proposed strategy provides the advantage of controlling the shape of the charging/discharging profile to match the general trend of solar PV power generation and peak load profile as compared to the traditional constant charging/discharging strategy. Therefore, in the midday when the PV impact is most severe, the proposed strategy can provide a better mitigation action as compared to the constant rate charging strategy. Similarly, the proposed strategy is able to provide a better voltage support during the occurrence of the maximum evening load compared to the constant rate discharging strategy. To account for the interventions in charging/discharging operation caused by any travel of the PEV, the proposed strategy adjusts the charging/discharging rates dynamically based on a reference SoC so that the limited available capacity of the PEV battery is utilized in a wise manner. Simulation results show that proposed strategy can provide better mitigation and voltage support as compared to a constant rate strategy. The simulation results also suggest that even when some PEVs in a feeder are not being plugged in at home, the remaining PEVs that are connected to the grid may still offer appreciable benefits in terms of solar PV impact mitigation and network voltage support. It is envisaged that the proposed strategy will provide some economic benefits, such as reducing the evening peak load and mitigating the PV impacts using synergetic PEV batteries. However, its financial implications need to be assessed based on the potential energy loss in the charging and discharging of the PEV batteries, its impact on the PEV battery's life-cycle, and the potential impact that electricity tariff can cause on the proposed strategy.

REFERENCES

[1] O. Erdinc, N. G. Paterakis, T. D. P. Mendes, A. G. Bakirtzis, and J. P. S. Catalao, "Smart household operation considering bi-directional EV and ESS utilization by real-time pricing-based DR," IEEE Trans. Smart Grid, vol. 6, no. 3, pp. 1281–1291, May 2015.
[2] J. M. Foster, G. Trevino, M. Kuss, and M. C. Caramanis, "Plug-in electric vehicle and voltage support for distributed solar: Theory and application," IEEE Syst. J., vol. 7, no. 4, pp. 881–888, Dec. 2013.
[3] L. Igualada, C. Corchero, M. Cruz-Zambrano, and F.-J. Heredia, "Optimal energy management for a residential microgrid including a vehicle-to-grid system," IEEE Trans. Smart Grid, vol. 5, no. 4, pp. 2163–2172, Jul. 2014.
[4] J. Lassila, J. Haakana, V. Tikka, and J. Partanen, "Methodology to analyze the economic effects of electric cars as energy storages," IEEE Trans. Smart Grid, vol. 3, no. 1, pp. 506–516, Mar. 2012.
[5] C. Pang, P. Dutta, and M. Kezunovic, "BEVs/PHEVs as dispersed energy storage for V2B uses in the smart grid," IEEE Trans. Smart Grid, vol. 3, no. 1, pp. 473–482, Mar. 2012.
[6] A. Y. Saber and G. K. Venayagamoorthy, "Plug-in vehicles and renewable energy sources for cost and emission reductions," IEEE Trans. Ind. Electron., vol. 58, no. 4, pp. 1229–1238, Apr. 2011.
[7] M. Singh, P. Kumar, and I. Kar, "A multi charging station for electric vehicles and its utilization for load management and the grid support," IEEE Trans. Smart Grid, vol. 4, no. 2, pp. 1026–1037, Jun. 2013.
[8] D. P. Tuttle and R. Baldick, "The evolution of plug-in electric vehiclegrid interactions," IEEE Trans. Smart Grid, vol. 3, no. 1, pp. 500–505, Mar. 2012.
[9] M. Yilmaz and P. T. Krein, "Review of the impact of vehicle-to-grid technologies on distribution systems and utility interfaces," IEEE Trans. Power Electron., vol. 28, no. 12, pp. 5673–5689, Dec. 2013.
[10] K. Clement-Nyns, E. Haesen, and J. Driesen, "The impact of charging plug-in hybrid electric vehicles on a residential distribution grid," IEEE Trans. Power Syst., vol. 25, no. 1, pp. 371–380, Feb. 2010.
[11] Q. Kejun, Z. Chengke, M. Allan, and Y. Yue, "Modeling of load demand due to EV battery charging in distribution systems," IEEE Trans. Power Syst., vol. 26, no. 2, pp. 802–810, May 2011.
[12] H. Sikai and D. Infield, "The impact of domestic plug-in hybrid electric vehicles on power distribution system loads," in Proc. Int. Conf. Power Syst. Technol. (POWERCON), Hangzhou, China, 2010, pp. 1–7.
[13] A. Canova, L. Giaccone, F. Spertino, and M. Tartaglia, "Electrical impact of photovoltaic plant in distributed network," IEEE Trans. Ind. Appl., vol. 45, no. 1, pp. 341–347, Jan./Feb. 2009.
[14] F. Spertino, P. D. Leo, and V. Cocina, "Which are the constraints to the photovoltaic grid-parity in the main European markets?" Sol. Energy, vol. 105, pp. 390–400, Jul. 2014.
[15] R. Tonkoski, L. A. C. Lopes, and T. H. M. El-Fouly, "Coordinated active power curtailment of grid connected PV inverters for overvoltage prevention," IEEE Trans. Sustain. Energy, vol. 2, no. 2, pp. 139–147, Apr. 2011.
[16] E. Demirok et al., "Local reactive power control methods for overvoltage prevention of distributed solar inverters in low-voltage grids," IEEE J. Photovolt., vol. 1, no. 2, pp. 174–182, Oct. 2011.
[17] J. Tomi´c and W. Kempton, "Using fleets of electric-drive vehicles for grid support," J. Power Sources, vol. 168, pp. 459–468, Jun. 2007.
[18] W. Di, D. C. Aliprantis, and K. Gkritza, "Electric energy and power consumption by light-duty plug-in electric vehicles," IEEE Trans. Power Syst., vol. 26, no. 2, pp. 738–746, May 2011.
[19] J. R. Aguero et al., "Integration of plug-in electric vehicles and distributed energy resources on power distribution systems," in Proc. IEEE Int. Elect. Vehicle Conf. (IEVC), Greenville, SC, USA, 2012, pp. 1–7.

[20] F. Marra et al., "EV charging facilities and their application in LV feeders with photovoltaics," IEEE Trans. Smart Grid, vol. 4, no. 3, pp. 1533–1540, Sep. 2013.
[21] F. Marra et al., "Improvement of local voltage in feeders with photovoltaic using electric vehicles," IEEE Trans. Power Syst., vol. 28, no. 3, pp. 3515–3516, Aug. 2013.
[22] M. J. E. Alam, K. M. Muttaqi, and D. Sutanto, "Mitigation of rooftop solar PV impacts and evening peak support by managing available capacity of distributed energy storage systems," IEEE Trans. Power Syst., vol. 28, no. 4, pp. 3874–3884, Nov. 2013.
[23] (10 Feb. 2014). 2011 Nissan Leaf – VIN 0356 Advanced Vehicle Testing – Beginning-of-Test Battery Testing Results. [Online]. Available: http://www1.eere.energy.gov/vehiclesandfuels/ avta/pdfs/fsev/battery_leaf_0356.pdf
[24] G. M. Masters, Renewable and Efficient Electric Power Systems. Hoboken, NJ, USA: Wiley, 2004.
[25] (2010). Eltek Valere Installation Guide: Electric Vehicle Power Chargers, 3kW HE. [Online]. Available: http://evolveelectrics.com/PDF/Eltek/Eltek%20Guide%20IP20.pdf
[26] J. Taylor, J. W. Smith, and R. Dugan, "Distribution modeling requirements for integration of PV, PEV, and storage in a smart grid environment," in Proc. IEEE Power Energy Soc. Gen. Meeting, San Diego, CA, USA, 2011, pp. 1–6.
[27] S. Wencong and C. Mo-Yuen, "Evaluation on intelligent energy management system for PHEVs/PEVs using Monte Carlo method," in 4th Int. Conf. Elect. Util. Dereg. Res. Power Tech., Weihai, Shandong, China, 2011, pp. 1675–1680.

AUTHOR DETAILS

Mr. VAKEEL SRIDHAR received a diploma in Electrical and Electronics Engineering from Vijay Rural Engineering College, Dasnagar (V), Nizamabad (D), Telangana, India, and received a B.Tech degree in EEE from Trinity College of Engineering and Technology, Bommakal (V), Karimnagar (D), Hyderabad, Telangana, India from JNTUH University in 2021. And Pursuing M.Tech in Electrical Power Systems at Holy Mary Institute of Technology and Science, Bogaram (V), Medchal (D), Hyderabad, Telangana, India, in the department of electrical and electronics engineering.

Mr. S RADHA KRISHNA REDDY received the B.Tech. in Electrical and Electronics Engineering from MITS Engineering College, Andhra Pradesh, India and M.Tech. in Power Electronics from S. K University, in 2007. He has 16.6 years of teaching experience, currently working as a Professor of Dept. of Electrical & Electronics Engineering at Holy Mary Institute of Technology and Science, Hyderabad, India and Pursuing PhD JNTU Hyderabad. He Published 48 research Papers. His research interests are Computer-aided power system analysis and modelling, wide area monitoring protection and control, Power Electronics, FACTS etc.

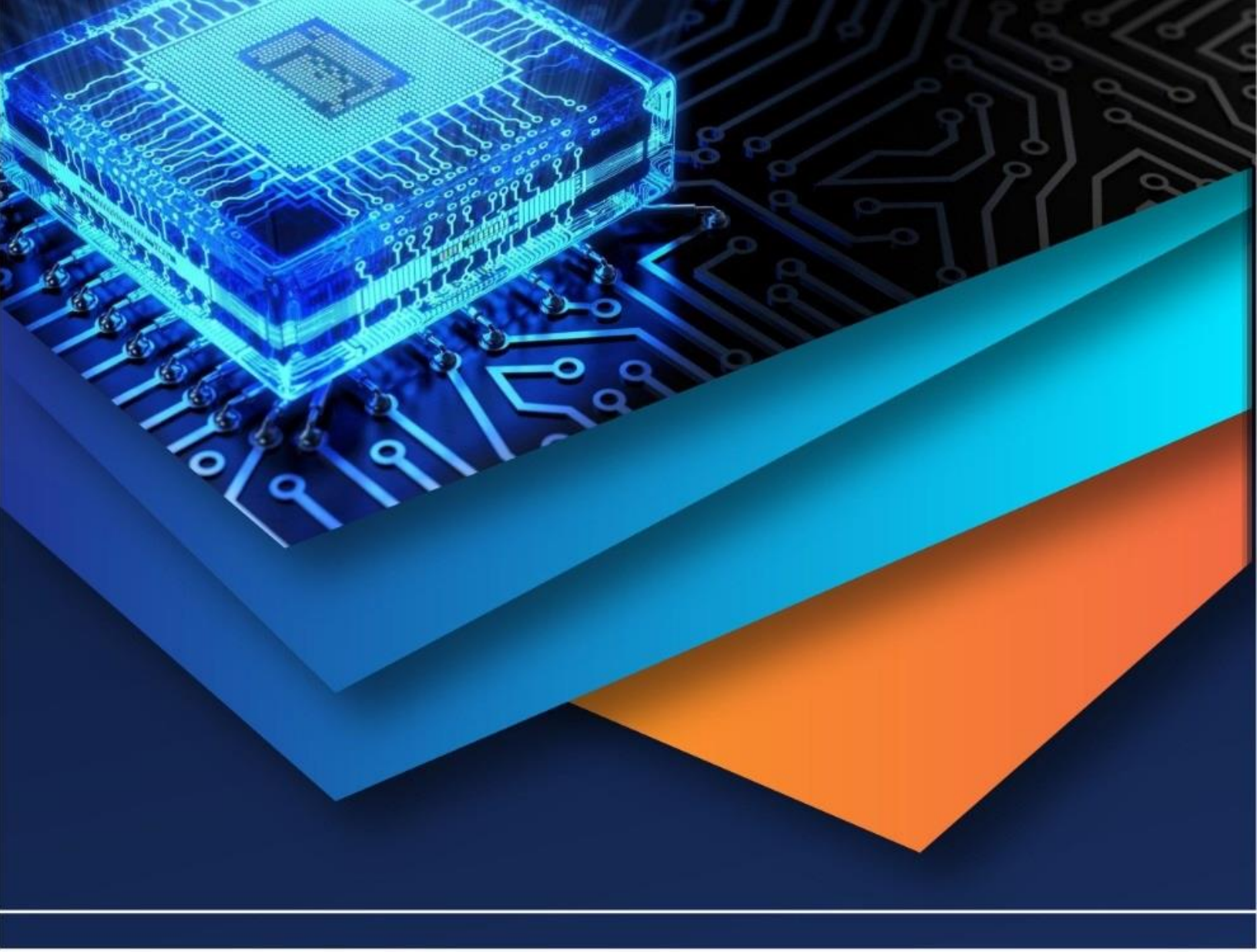

10.22214/IJRASET

45.98

IMPACT FACTOR: 7.129

IMPACT FACTOR: 7.429

INTERNATIONAL JOURNAL FOR RESEARCH

IN APPLIED SCIENCE & ENGINEERING TECHNOLOGY